 SDHM, vol.2, no.2, pp.123-130, 2006

The Use of the Tangential Differential Operator in the Dual Boundary Element Equation

L. Palermo Jr.[1], **L.P.C.P.F. Almeida**[2], **and P.C. Gonçalves**[3]

Abstract: The kernels of integrands are usually differentiated to obtain the general boundary integral equation (BIE) for stresses and its corresponding traction equation. An alternative BIE for stresses can be obtained when the tangential differential operator is introduced in problems using Kelvin type fundamental solutions. The order of the singularity is reduced with this strategy and the Cauchy principal value sense or the first order regularization can be used in the resultant BIE. The dual boundary element formulation with the BIE for tractions using the tangential differential operator is analyzed in the present study. Shape functions with same expressions for conformal or non-conformal interpolations are adopted and conformal interpolations were applied on the crack surface without losing the accuracy of the dual formulation. The results obtained are compared with solutions available from the literature to evaluate the formulation.

keyword: Tangential Differential Operator, Dual Boundary Element Method, Stress Intensity Factor.

1 Introduction

Accurate values for stresses at the boundary may be evaluated with the stress boundary integral equation (BIE) [Guiggiani (1994)]. Nevertheless, the differentiation of the kernels of integrals in the displacement BIE to obtain an equation for stresses increases the order of the kernel singularity and an additional care is necessary to treat the improper integrals. The use of the tangential differential operator (TDO) in the stress BIE is an interesting procedure when Kelvin type fundamental solutions are employed and the reduction of the order of the kernel singularity is the main benefit [Bonnet (1999), Kupradze (1979), Sladek and Sladek (1983)]. A short explanation on how to obtain the TDO in the stress BIE will be presented next. The BIE for the gradient at an internal point x can be written using the differentiation in terms of field variables:

$$u_{i,m}(x) = \int_\Gamma T_{ij,m}(x,y)\ u_j(y)\ d\Gamma(y) - \int_\Gamma U_{ij,m}(x,y)\ t_j(y)\ d\Gamma(y) \tag{1}$$

U_{ij} (x, y) and T_{ij} (x, y) are the displacement and the traction, respectively, in the direction j at the boundary point y due to a singular load in the direction i at the collocation point x, according to the Kelvin solution; u_j(y) and t_j(y) are the displacement and the traction at the field point, respectively.

The first and the second integrals of equation (1) are regular for internal points and exhibit singularities of order $1/r^2$ and $1/r$ in two dimensional problems, respectively, when the field point approaches the collocation point. The TDO can be introduced in the first integral of the right member of equation (1) and the following relations are obtained:

$$\int_\Gamma T_{ij,m}(x,y)\ u_j(y)\ d\Gamma(y) = \int_\Gamma n_b(y)\ \sigma_{ibj,m}(x,y)\ u_j(y)\ d\Gamma(y) \tag{2}$$

$$\int_\Gamma n_b(y)\ \sigma_{ibj,m}(x,y)\ u_j(y)\ d\Gamma(y) = \int_\Gamma \left\{D_{bm}\left[\sigma_{ibj}(x,y)\right] + n_m(y)\ \sigma_{ibj,b}(x,y)\right\} u_j(y)\ d\Gamma(y) \tag{3}$$

$D_{bm}(\ )$ is the tangential differential operator, which has the following definition:

$$D_{bm}[f(y)] = n_b(y)\ f_{,m}(y) - n_m(y)\ f_{,b}(y) \tag{4}$$

[1] FEC/UNICAMP, Campinas, SP, Brazil – leandro@fec.unicamp.br
[2] FEC/UNICAMP, Campinas, SP, Brazil
[3] FEC/UNICAMP, Campinas, SP, Brazil

The second term in the integral of the right member of equation (3) is turned null at points y not coincident with x (y≠x) when the Kelvin solution is used. The application of the integration by parts on the resultant term of the integral of the right member of equation (3) yields, [Bonnet (1999)]:

$$\int_{\Gamma} D_{bm}\left[\sigma_{ibj}(x,y)\right]\, u_j(y)\; d\Gamma(y) = \int_{\Gamma} \sigma_{ibj}(x,y)\; D_{mb}\left[u_j(y)\right] d\Gamma(y) \tag{5}$$

The BIE for the gradient using the TDO has the following expression:

$$u_{i,m}(x) = \int_{\Gamma} \sigma_{ibj}(x,y)\; D_{mb}\left[u_j(y)\right] d\Gamma(y) - \int_{\Gamma} U_{ij,m}(x,y)\; t_j(y)\; d\Gamma(y) \tag{6}$$

The integrals of equation (6) are regular for internal points and exhibit singularities of order 1/r when the field point approaches the collocation point. The BIE for stress can be obtained from equations (1) or (6) using the Hooke tensor and the symmetry property of $U_{ij,m}$ (x, y):

$$\sigma_{ak}(x) = C_{\text{akim}} \int_{\Gamma} T_{ij,m}(x,y)\; u_j(y)\; d\Gamma(y) - \int_{\Gamma} \sigma_{jak}(x,y)\; t_j(y)\; d\Gamma(y) \tag{7}$$

$$\sigma_{ak}(x) = C_{\text{akim}} \int_{\Gamma} \sigma_{ibj}(x,y)\; D_{mb}\left[u_j(y)\right] d\Gamma(y) - \int_{\Gamma} \sigma_{jak}(x,y)\; t_j(y)\; d\Gamma(y) \tag{8}$$

$$C_{akim} = \mu\left(\frac{2\nu}{1-2\nu}\delta_{ak}\delta_{im} + \delta_{ai}\delta_{km} + \delta_{am}\delta_{ki}\right) \tag{9}$$

C_{akim} is the Hooke tensor for isotropic media, ν is the Poisson ratio, μ is the shear modulus and δ_{ij} is the Kronecker delta.

The stress BIE at a boundary point is defined as the limiting form of the corresponding BIE at an internal point when it is led to a point on the boundary. For a point x' on a smooth boundary, equations (7) and (8) can now be written as:

$$\frac{1}{2}\sigma_{ak}(x') = C_{\text{akim}} \int_{\Gamma} T_{ij,m}(x',y)\; u_j(y)\; d\Gamma(y) - \int_{\Gamma} \sigma_{jak}(x',y)\; t_j(y)\; d\Gamma(y) \tag{10}$$

$$\frac{1}{2}\sigma_{ak}(x') = C_{\text{akim}} \int_{\Gamma} \sigma_{ibj}(x',y)\; D_{mb}\left[u_j(y)\right] d\Gamma(y) - \int_{\Gamma} \sigma_{jak}(x',y)\; t_j(y)\; d\Gamma(y) \tag{11}$$

It is important to note on the continuity requirement for the derivative of the displacement function at the collocation point x'. The traction BIE is obtained from equation (10) or (11) when the stress tensor obtained at the boundary point x' is multiplied by direction cosines of the outward normal at this point (n'), i.e.:

$$\frac{1}{2}t_k(x') = n'_a(x')\, C_{\text{akim}} \int_{\Gamma} T_{ij,m}(x',y)\; u_j(y)\; d\Gamma(y) - n'_a(x') \int_{\Gamma} \sigma_{jak}(x',y)\; t_j(y)\; d\Gamma(y) \tag{12}$$

$$\frac{1}{2}t_k(x') = n'_a(x')\, C_{\text{akim}} \int_{\Gamma} \sigma_{ibj}(x',y)\; D_{mb}\left[u_j(y)\right] d\Gamma(y) - n'_a(x') \int_{\Gamma} \sigma_{jak}(x',y)\; t_j(y)\; d\Gamma(y) \tag{13}$$

2 The Dual Boundary Integral Equations

Several strategies have been employed to analyze crack problems such as the displacement discontinuity method [Crouch (1976); Wen (1996)], the crack Green's function method [Snyder (1975)], the numerical Green's function method [Guimarães and Telles (2000)], the subregion (or subdomain) method [Blandford, Ingraffea and Liggett (1976)] and the dual boundary element method (DBEM) [Portela, Aliabadi and Rooke (1992); Mi and Aliabadi (1992); Chen and Chen (1995)]. A detailed review on the boundary formulations in fracture mechanics was presented in [Aliabadi (1997)]. The displacement and the traction BIE are the equations employed in DBEM. The

equation (12) is the well-known BIE for tractions and the displacement BIE has the following expression for the collocation point x' on a smooth boundary:

$$\frac{1}{2}u_i\left(x'\right)+\int_{\Gamma} T_{ij}\left(x',y\right)u_j\left(y\right)d\Gamma\left(y\right) = \int_{\Gamma} U_{ij}\left(x',y\right)t_j\left(y\right)d\Gamma\left(y\right) \tag{14}$$

When the displacement BIE is applied to one of the crack surfaces and the traction equation to the other, general mixed-mode crack problems can be solved with a single domain formulation. Although the integration path is still the same for coincident points on the crack surfaces, the respective boundary integral equations are now distinct. The collocation point needed to perform the traction boundary integral equation and the strategy used to treat improper integrals are the essential features of the formulation.

The collocation points must be positioned to satisfy the continuity requirements for each BIE. The continuity of the displacement function at x' is the necessary condition for the displacement BIE whereas the continuity of the displacement derivative is required for the traction BIE. These conditions are generally satisfied for collocation points placed in the interior of the boundary element. The collocation points may be placed at the ends of the element when the shape functions, which approximate displacements and derivatives in the element, satisfy the necessary conditions at these points [Portela, Aliabadi and Rooke (1992), Bonnet (1999)].

The integrals of equation (14) are regular for internal points and exhibit singularities of order 1/r and ln(1/r), in two dimensional problems, for points on the boundary. The improper integrals can be handled by the classical singularity subtraction method and the natural definition of ordinary finite-part integrals is reached, as detailed explained in [Portela, Aliabadi and Rooke (1992)]. Analytical expressions can be used to evaluate the singular integral and the Gauss-Legendre scheme is employed for the regular integral. The local parametric co-ordinate ξ is defined in the range (-1, 1) and the collocation point position is ξ'. The displacement components u_j are approximated in the local co-ordinate system in terms of nodal values u_j^n. The first order finite-part integral expressed in the local co-ordinate ξ is:

$$\int_{\Gamma e} T_{ij}\left(x',y\right)u_j\left(y\right)d\Gamma\left(y\right) = u_j^n\left[\int_{-1}^{+1}\frac{f_{ij}^n\left(\xi\right)-f_{ij}^n\left(\xi'\right)}{\xi-\xi'}d\xi+f_{ij}^n\left(\xi'\right)\int_{-1}^{+1}\frac{d\xi}{\xi-\xi'}\right] \tag{15}$$

The regular function $f_{ij}^n(\xi)$ is given by the product of the fundamental solution, the shape function, the Jacobian of the co-ordinate transformation and the term $(\xi-\xi')$. The first integral of the right hand side of equation (15) is regular and the second can be integrated analytically [Portela, Aliabadi and Rooke (1992)].

The order of singularities in the traction BIE with TDO (equation 13) is 1/r in both integrals. The improper integrals can be treated with the first order finite part as shown in equation (15) for the singular kernel of the displacement BIE. The regular function derived from the kernel containing TDO is given by the product of the kernel and the term ($\xi\xi$'). A detailed explanation on the algebraic manipulation of the kernel containing TDO, when it is written in terms of local coordinates, is presented in [Bonnet (1999)].

3 Boundary Elements and Internal Collocation Points

Linear shape functions were employed to approximate displacements and efforts in the boundary elements. The same shape function was used for conformal and non-conformal interpolations with nodal parameters positioned at the ends of the elements. The collocation points were shifted to the interior of the element at a distance of a six part of its length from the end. The collocation point position (ξ'), in the range (-1, 1), was: i) ξ'=-0.67 for continuous elements; ii) ξ'=-0.67 and ξ'=+0.67 for discontinuous elements. The number of collocation points in the element was defined by the computer code according to the condition of the last node, which means that an element with the discontinuity at the first node had one collocation point. The present numerical implementation was studied in [Almeida and Palermo (2004)] with equations (12) and (14) in the dual formulation. The use of conformal interpolations along the crack surfaces without losing the accuracy of the dual formulation was the main feature shown in that study.

The dual formulation with TDO in the traction BIE is analyzed in this paper. The derivatives of the adopted shape function for displacements (linear functions) are used in the traction equation, as required for the TDO, and constant values with opposite signs were obtained for the tangent derivatives. The background purpose was the analysis of the TDO using derivatives of a low order shape function.

The traction BIE with TDO was employed for collocation points positioned on one of the crack surfaces whereas other positions used the displacement BIE as it was done with equations (12) and (14) in [Portela, Aliabadi and Rooke (1992); Almeida and Palermo (2004)]. The diagonal terms were obtained directly using the collocation point position on the element and the shape function.

The use of non-conformal interpolations required a revision of the result obtained from equation (5) and the effect of the ends from the integration by parts had to be considered. The integration by parts presented in equation (5) is repeated next and the effect of the ends is included:

$$\int_{\Gamma e} D_{bm}\left[\sigma_{ibj}(x,y)\right]\, u_j(y)\; d\Gamma(y) = \left[e_{3bm}\sigma_{ibj}(x,y)\, u_j(y)\right]_0^{\Gamma e} + \int_{\Gamma e} \sigma_{ibj}(x,y)\; D_{mb}\left[u_j(y)\right]\, d\Gamma(y) \tag{16}$$

Γ_e is an open line, e_{ijk} is the permutation symbol.

The equation (11) can be rewritten including the effect of the ends in case of discontinuity in displacements at one point:

$$\frac{1}{2}\sigma_{ak}(x') = C_{\text{akim}} \int_{\Gamma} \sigma_{ibj}(x',y)\; D_{mb}\left[u_j(y)\right]\, d\Gamma(y) - \int_{\Gamma} \sigma_{iak}(x',y)\; t_j(y)\; d\Gamma(y) + C_{\text{akim}} e_{3bm}\sigma_{ibj}(x,y)\left[u_j^B(y) - u_j^F(y)\right]. \tag{17}$$

The term between brackets of equation (16) appeared in equation (17) as a multiplier of displacements u_j^B and u_j^F, which are at the backward and at the forward side of the discontinuity respectively. It is important to note that u_j^B and u_j^F have the same geometrical coordinates according to the presented strategy for the non-conformal interpolation.

4 Stress Intensity Factor Evaluation

The near-tip displacement extrapolation is used to obtain stress intensity factors as explained in [Portela, Aliabadi and Rooke (1992), Almeida and Palermo (2004)]. Consider a polar coordinate system (r, θ) centered at the crack tip, such that the crack surfaces could be defined with $\theta = \pm\pi$. The displacement field on the crack surface is written next and considering the first term of William's expansion:

$$u_2(\theta=\pi) - u_2(\theta=-\pi) = \frac{\kappa+1}{\mu} K_I \sqrt{\frac{r}{2\pi}} \tag{18}$$

$$u_1(\theta=\pi) - u_1(\theta=-\pi) = \frac{\kappa+1}{\mu} K_{II} \sqrt{\frac{r}{2\pi}} \tag{19}$$

The stress intensity factors for deformation modes II and I are K_{II} and K_I, respectively, the parameter κ is equal to 3-4η; η is equal to ν for plane strain problems and equal to ν/(1+ν) for plane stress problems. The near-tip displacement extrapolation works with equations (18) and (19) to obtain the stress intensity factors when the displacements are known. The situation is shown in Figure 1, where opposite linear elements share the crack tip at nodes B and C.

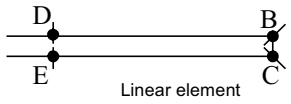

Figure 1 : Crack tip at points B and C.

The length of the linear element is equal to l. The expressions for the stress intensity factors are given by:

$$K_I^{DE} = \left(u_2^D - u_2^E\right).\frac{\mu}{\kappa+1}.\sqrt{2}.\sqrt{\frac{\pi}{l}} \tag{20}$$

$$K_{II}^{DE} = \left(u_1^D - u_1^E\right).\frac{\mu}{\kappa+1}.\sqrt{2}.\sqrt{\frac{\pi}{l}} \tag{21}$$

5 Numerical Example

Three cases were studied using linear boundary elements and a conformal interpolation on the crack surfaces. Double nodes were introduced at corners and at crack tips. The results obtained with equations (13) and (14) were compared to the literature and boundary element formulations using equations (12) and (14).

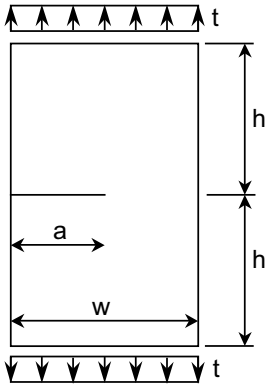

Figure 2 : Single edge crack

A non-conformal interpolation with quadratic functions was employed in [Portela, Aliabadi and Rooke (1992)] and the results were picked from those using near-tip displacement extrapolation. The results derived from [Almeida and Palermo (2004)] were obtained with the same mesh adopted in this study.

A rectangular plate containing a single horizontal edge crack shown in Figure 2 used a mesh with 48 linear elements plus 8 elements on each crack surface (64 B.E.). The crack length is a, the plate width is w and the height is 2h. A uniform traction in the height direction was symmetrically applied at the ends. Results obtained for the ratio h/w equals to 0.5 are shown in Table 1. Three ratios a/w were considered: 0.2, 0.4, and 0.6. The stress intensity factor was obtained with equation (20).

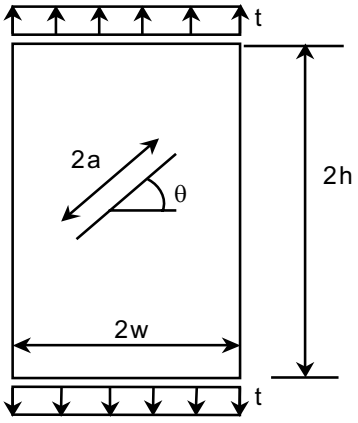

Figure 3 : Central Slant Crack (θ=45 $^\circ$)

A rectangular plate containing a central slant crack shown in Figure 3 had a mesh with 48 linear elements plus 12 elements on each crack surface (72 B.E.). The crack length is 2a, the plate width is 2w and the height is 2h. A uniform traction in the height direction was symmetrically applied at the ends. Results obtained for the h/w ratio equal to 2 are shown in Tables 2 and 3. Three ratios a/w were considered: 0.2, 0.4, and 0.6. The stress intensity factors were obtained with equations (20) and (21).

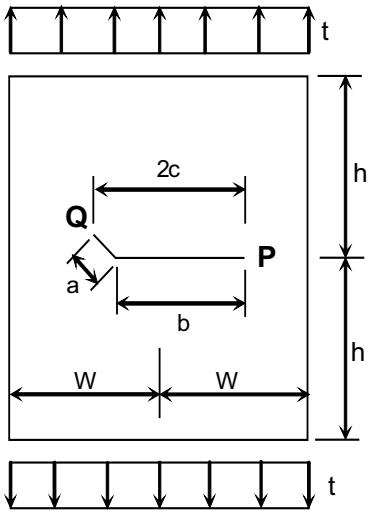

Figure 4 : Central Kinked Crack

A rectangular plate containing an internal kinked crack shown in Figure 4 had a mesh with 60 linear elements plus 10 elements on each horizontal crack surface and 8 elements on each inclined crack surface (96 B.E.). One of the segments of the crack is horizontal with length b while the other segment makes an angle of 45 degrees with the horizontal and has length a; the horizontal projection of the total crack is given by $2c = b + a\frac{\sqrt{2}}{2}$. The kink of the crack is at the center of the plate, the plate width is 2w and the height is 2h. Three ratios (a/b) were considered: 0.2, 0.4 and 0.6. The results obtained for b/w equal to 0.1 and h/w equal to 2 are shown in Tables 4 to 7. Stress intensity factors were obtained with equations (20) and (21).

The values obtained with TDO for stress intensity factors were not significantly changed with reference to those presented in Almeida and Palermo (2004) where the traction BIE used the equation (12). The stress intensity factors were calculated using differences in displacements of opposite nodes on the crack surfaces. The results

Table 1 : Results for the single edge crack with 64 linear elements: $K_I/\left(t\sqrt{\pi a}\right)$

(1)	(2)	(3)	(4)	(5)	(%)
a/w	Civilek and Erdogan (1982)	Portela, Aliabadi and Rooke (1992)	Almeida and Palermo (2004)	TDO	$\left\|\frac{(2)-(5)}{(2)}\right\|$
0.2	1.488	1.566	1.496	1.501	0.87
0.4	2.324	2.230	2.383	2.368	1.89
0.6	4.152	4.580	4.355	4.254	2.46

Table 2 : Results for the central slant crack with 72 linear elements: $K_I/\left(t\sqrt{\pi a}\right)$

(1)	(2)	(3)	(4)	(5)	(%)
a/w	Murakami (1987)	Portela, Aliabadi and Rooke (1992)	Almeida and Palermo (2004)	TDO	$\left\|\frac{(2)-(5)}{(2)}\right\|$
0.2	0.518	0.531	0.513	0.513	0.97
0.4	0.572	0.588	0.567	0.567	0.87
0.6	0.661	0.686	0.660	0.660	0.15

Table 3 : Results for the central slant crack with 72 linear elements: $K_{II}/\left(t\sqrt{\pi a}\right)$

(1)	(2)	(3)	(4)	(5)	(%)
a/w	Murakami (1987)	Portela, Aliabadi and Rooke (1992)	Almeida and Palermo (2004)	TDO	$\left\|\frac{(2)-(5)}{(2)}\right\|$
0.2	0.507	0.519	0.502	0.502	1.0
0.4	0.529	0.541	0.524	0.523	1.15
0.6	0.567	0.579	0.561	0.561	1.06

Table 4 : Results for the kinked crack at P with 96 linear elements: $K_I/\left(t\sqrt{\pi c}\right)$

(1)	(2)	(3)	(4)	(5)	(%)
a/b	Murakami (1987)	Portela, Aliabadi and Rooke (1992)	Almeida and Palermo (2004)	TDO	$\left\|\frac{(2)-(5)}{(2)}\right\|$
0.2	0.995	1.021	0.988	0.988	0.71
0.4	0.990	1.018	0.985	0.985	0.51
0.6	0.986	1.017	0.983	0.983	0.31

Table 5 : Results for the kinked crack at P with 96 linear elements: $K_{II}/\left(t\sqrt{\pi c}\right)$

(1)	(2)	(3)	(4)	(5)	(%)
a/b	Murakami (1987)	Portela, Aliabadi and Rooke (1992)	Almeida and Palermo (2004)	TDO	$\left\|\frac{(2)-(5)}{(2)}\right\|$
0.2	0.028	0.030	0.029	0.029	3.57
0.4	0.033	0.036	0.035	0.035	6,1
0.6	0.030	0.032	0.032	0.032	6.67

Table 6 : Results for the kinked crack at Q with 96 linear elements: $K_I/\left(t\sqrt{\pi c}\right)$

(1)	(2)	(3)	(4)	(5)	(%)
a/b	Murakami (1987)	Portela, Aliabadi and Rooke (1992)	Almeida and Palermo (2004)	TDO	$\left\|\frac{(2)-(5)}{(2)}\right\|$
0.2	0.598	0.634	0.636	0.636	6.35
0.4	0.574	0.603	0.606	0.606	5.57
0.6	0.568	0.595	0.600	0.600	5.63

Table 7 : Results for the kinked crack at Q with 96 linear elements: $K_{II}/\left(t\sqrt{\pi c}\right)$

(1)	(2)	(3)	(4)	(5)	(%)
a/b	Murakami (1987)	Portela, Aliabadi and Rooke (1992)	Almeida and Palermo (2004)	TDO	$\left\|\frac{(2)-(5)}{(2)}\right\|$
0.2	0.557	0.589	0.590	0.590	5.92
0.4	0.607	0.637	0.639	0.639	5.27
0.6	0.627	0.659	0.661	0.661	5.42

showed that the precision obtained for displacements was not affected by the partial regularization introduced by the integration by parts (equation 5 or 16) and the derivatives of the shape function for displacements in the TDO. On the other hand, the results using TDO were close to those presented by Civilek and Erdogan (1982) or Murakami (1987) and the deviations were greater for values of the internal kinked crack. It is important to note that better values for stress intensity factors can be obtained with J-integral technique. The J-integral technique was used in Portela, Aliabadi and Rooke (1992) where its benefit was shown.

6 Conclusions

The numerical results obtained were close to values from the literature. A minimum difference was noted in the results presented in [Portela, Aliabadi and Rooke (1992); Almeida and Palermo (2004)] and those obtained using the TDO, which have the benefit of the reduction of the order of the singularity. The use of derivatives of the adopted shape function for displacement without using other interpolation for TDO was an interesting alternative. It is important to note that constant values were obtained as derivatives of the linear shape function and the results were not degraded. Regarding the present numerical implementation, a conformal interpolation on the crack surface was used without losing the accuracy of the dual formulation even considering that the BIE for traction employed the TDO on low order elements.

References

Aliabadi, M.H. (1997): Boundary element formulations in fracture mechanics, *Appl. Mech. Rev*., 50 , 83-96.

Almeida, L.P.C.P.F.; Palermo Jr., L. (2004): On the Implementation of the Two Dimensional Dual Boundary Element Method for Crack Problems, *5th Int. Conference on Boundary Elements Techniques*, Lisboa, Portugal.

Blandford, G.E.; Ingraffea, T.A.; Liggett, J.A. (1976): Two-dimensional stress intensity factor computations using the boundary element method, *International Journal of Numerical Methods in Engineering*, 17, 387-404.

Bonnet, M. (1999): *Boundary Integral Equation Methods for Solids and Fluids*, John Wiley & Sons Ltd.

Chen, W.H.; Chen, T.C. (1995): An efficient dual boundary element technique for a two-dimensional fracture problem with multiple cracks. *International Journal of Numerical Methods in Engineering*, 38, 1739-1756.

Civelek, M.B.; Erdogan, F. (1982): Crack problems for a rectangular sheet and an infinite strip, *International Journal of Fracture*, vol.19, pp. 139-159.

Crouch, S.L. (1976): Solution of plane elasticity problems by the displacement discontinuity method, *International Journal of Numerical Methods in Engineering*, 10, 301-342, 1976.

Guiggiani, M. (1994): Hypersingular formulation for boundary stresses evaluation. *Eng. Anal. Bound. Elem*., 14, 169-179.

Guimarães, S.; Telles, J.C.F. (2000): General application of numerical Green's functions for SIF computations with boundary elements, *CMES – Computer Modeling in Engineering & Sciences*, v. 1, 131-139.

Kupradze, V.D. (1979): *Three-dimensional problems of the mathematical theory of elasticity and thermoelasticity*. North Holand.

Mi, Y.; Aliabadi, M.H. (1992): Dual boundary element method for three-dimensional fracture mechanics analysis, *Eng. Anal. Bound. Elem*., 10, 161-171.

Murakami, Y. (1987): *Stress Intensity Factors Handbook*, Pergamon Press, Oxford.

Portela, A.; Aliabadi, M.H.; Rooke, D.P. (1992): The dual boundary element method: Effective implementation for crack problems, *International Journal of Numer-*

ical Methods in Engineering, 33, 1269-1287, 1992.

Sladek, J.; Sladek, V. (1983): Three-dimensional curved crack in an elastic body, *Int. J. Solids Struct*., 19, 425-436.

Snyder, M. D.; Cruse, T. A. (1975): Boundary integral equation analysis of cracked anisotropic plates, *International Journal of Fracture*, 11, 315-342.

Wen, P.H. (1996): *Dynamic fracture mechanics: displacement discontinuity method*, Computational Mechanics Publications.